

Optimizing Low-Dose [¹⁸F]FDG-PET/CT Scans: Ensuring Quality Amid Radiotracer Availability Challenges – Insights from a Peripheral Tertiary Care Center

Abstract

Background: The introduction of positron emission tomography/computed tomography (PET/CT) has significantly advanced medical imaging. In oncology, ¹⁸F-fluorodeoxyglucose (¹⁸F-FDG) PET/CT is particularly crucial for staging, evaluating treatment response, monitoring follow-up, and planning radiotherapy. However, in resource limiting hospitals, the availability of fluorine-labeled ¹⁸F-FDG limits optimal scan acquisition. This study aims to determine the optimal dosage and acquisition time to maximize patient throughput during shortages. **Aim and Objective:** To optimize low-dose ¹⁸F-FDG scan protocols while maintaining high image quality despite radiotracer availability challenges. **Materials and Methods:** PET/CT scans were performed using GE's Discovery IQ 5-ring, 16-slice system within 40–60 minutes of intravenous ¹⁸F-FDG injection. The protocol was adjusted to a low-dose (0.05 mCi/kg of ¹⁸F-FDG), and the PET data acquisition time was increased to 3 min per bed position to ensure image quality. **Results:** Notable differences were observed in image quality scores based on varying acquisition times, with the extended acquisition time helping maintain diagnostic standards despite reduced tracer doses. **Conclusion:** The high sensitivity and long axial length of the PET/CT system (with five rings spanning 26 cm AFOV) can significantly alleviate the challenges faced by cyclotron-dependent centers. By leveraging the increased sensitivity, we successfully reduced the injected activity rather than the scan time to address the tracer shortage at our institute. This approach proved to be effective in maintaining image quality and patient care standards.

Keywords: ¹⁸F-fluorodeoxyglucose, image and dose optimization, positron emission tomography-computed tomography

Introduction

The advent of positron emission tomography/computed tomography (PET/CT) in medicine has been a revolutionary development. The use of ¹⁸F-fluorodeoxyglucose (¹⁸F-FDG) in PET for metabolic assessment has become crucial in disease management.^[1] Specifically in oncology, ¹⁸F-FDG PET/CT is essential for staging, evaluation of treatment response, monitoring follow-up, and planning radiotherapy.^[2,3] Several technological advancements, such as the application of point spread function correction technology, replacement of conventional photomultiplier tubes with silicon photomultipliers in digital PET/CT, and improvement in the design of detectors have been made to improve the sensitivity of the scanner and the quality of imaging.^[4-10] Despite advancements in

technology (both hardware and software), the rate-limiting factor for optimal scan acquisition in Tier II city hospitals remains the availability of fluorine-labeled ¹⁸F-FDG, which is produced in medical cyclotron facilities. Very few centers in Tier II cities of India have a medical cyclotron facility nearby to ensure timely supply of ¹⁸F-FDG for PET-CT imaging. Reliance on long-distance road or air transport for delivering the radiopharmaceutical often results in its unavailability, causing inconvenience to patients and doctors and many times leading to delays in management. In addition to the high volume of patients, institutes in Tier II towns, face additional challenges of meeting the cost-efficiency of running a nuclear medicine department amidst the abruptness and inconvenience of radiotracer supply. Therefore, we decided to initiate a study to

**Sachin Tayal,
Yash Jain,
Sonali Thakur,
Varun Shukla,
Manikandan
Marappagounder
Venkatachalam,
Ajay Kumar,
Ritwik Sinha**

*Department of Nuclear
Medicine and Molecular
Imaging, Homi Bhabha Cancer
Hospital & Mahamana Pandit
Madan Mohan Malaviya Cancer
Centre, Tata Memorial Centre,
Homi Bhabha National Institute
(HBNI), Varanasi, India*

Address for correspondence:

Mr. Sachin Tayal,
Mahamana Pandit Madan
Mohan Malaviya Cancer
Centre, A Unit of Tata Memorial
Centre, BHU Campus, Sundar
Bagiya, Varanasi - 221 005,
Uttar Pradesh, India.
E-mail: sachintayal7@gmail.
com

Received: 24-06-2024

Revised: 31-08-2024

Accepted: 10-09-2024

Published: 18-11-2024

Access this article online

Website:

<https://journals.lww.com/ijnm>

DOI: 10.4103/ijnm.ijnm_90_24

Quick Response Code:



How to cite this article: Tayal S, Jain Y, Thakur S, Shukla V, Venkatachalam MM, Kumar A, et al. Optimizing low-dose [¹⁸F]FDG-PET/CT scans: Ensuring quality amid radiotracer availability challenges – Insights from a peripheral tertiary care center. Indian J Nucl Med 2024;39:292-8.

This is an open access journal, and articles are distributed under the terms of the Creative Commons Attribution-NonCommercial-ShareAlike 4.0 License, which allows others to remix, tweak, and build upon the work non-commercially, as long as appropriate credit is given and the new creations are licensed under the identical terms.

For reprints contact: WKHLRPMedknow_reprints@wolterskluwer.com

assess the optimum dosage and acquisition time to serve the maximum number of patients as effectively as possible during shortages. This study utilized GE's Discovery IQ 5 ring PET scanning system, featuring an axial field of view (FOV) of 26 cm per bed position, resulting in 79 imaging planes with a slice thickness of 27 mm and a sensitivity of 22 cps/kBq.^[11-14] Equipped with a bismuth germanium oxide (BGO) detector, this system achieves the highest sensitivity ever recorded by any nondigital PET system and comes at an affordable price.^[15] The modality employs Q Clear as the PET reconstruction algorithm, which is the commercial name for the Bayesian penalized likelihood reconstruction algorithm.^[16] This includes point spread function modeling and a noise suppression function, aided by a penalty term (β).

Materials and Methods

This is a retrospective study wherein patients' databases were evaluated from November 2022 to December 2023 at Mahamana Pandit Madan Mohan Malaviya Cancer Centre, Varanasi, A Unit of Tata Memorial Centre. Patients presenting with clinical indications such as multiple myeloma, sarcoma, fever of unknown origin, or metastases of unknown primary, which necessitate imaging of the bilateral lower limbs, were excluded from the study due to limitations in available activity and time constraints. All these patients had undergone clinical PET-CT study at our institute during limited radiotracer availability. Hence, they were adjusted with low-dose protocol: 0.05 mCi/kg was injected intravenously and acquisition of PET data was increased to 3 min/bed for keeping their image quality uncompromised. The demographic and clinical information of 40 enrolled patients are summarized in Table 1. Most of the patients selected were 150–160 cm in length restricting the scan length to be covered under 4 bed positions. Out of 40 patients, 21 were male and 19 were female, with a mean

age of 51 ± 15.3 years and mean body mass index (BMI) of 20.4 ± 3.7 kg/m². Among 40 patients, the BMI of 19 patients was in the range 18–25 kg/m², followed by 14 patients with <18 kg/m², and only 7 with >25 kg/m². The mean preinjected dose was 2.6 ± 0.5 mCi, post injected dose was 0.1 ± 0.06 mCi, resulting in a net injected dose being 2.5 ± 0.5 mCi, as shown in Figure 1. All patients were asked to be on fasting for at least 6 h before the study. Patients with fasting blood sugar concentration >170 mg/dL were excluded from the study. Scan was acquired on GE's Discovery IQ 5 ring, 16-slice PET/CT, within 40–60 min after injecting ^{18}F -FDG intravenously. Each ring in PET assembly has 36 detector units, wherein each unit consists of 6.3 mm \times 6.3 mm \times 30 mm BGO crystal, with an 8 \times 8-matrix configuration. These are further supported by 720 photomultipliers in total. Patients were imaged in supine position, arms stretched up/down as per the clinical case and asked to maintain shallow respiration during the study. A scout image, followed by a contrast-enhanced CT and finally PET data were acquired. PET images were acquired in three-dimensional list mode from the skull to mid-thigh. CT served dual purpose: attenuation correction of PET data and for image fusion. Recon matrix of 192 \times 192 was used and the algorithm-Q clear with 4 iterations and 12 subsets was applied. Q clear algorithm uses regularization to reduce noise. The β parameter with larger values was used for increasing noise reduction, with β value equal to 350 as the default value (company setting). Two new series of PET images in addition were created retrospectively from the generated raw sinogram datasets of 3 min/bed: 2 min/bed and 1 min/bed respectively for comparison of all the three different time/bed data. In total, 120 scans (3 scans per patient) were reviewed by two experienced nuclear medicine physicians and images scored qualitatively using a 5-point Likert scale (1 = unacceptable image quality; 2 = poor image quality; 3 = acceptable image; 4 = good image quality; and 5 = excellent image quality). In addition to this, quantitative assessment was done by drawing a region of interest in the right liver lobe on a 3 min/bed image and the same was copied to the other two sets of respectively reconstructed data. Maximum standardized uptake value (SUV_{max}) and mean SUV (SUV_{mean}) and standard deviation were measured between the three data sets. Images were reviewed using a dedicated workstation with three PET datasets opened and linked automatically for simultaneous assessment. The order of image data was randomized to reduce biases. Second, both the readers were blinded to scan dose and acquisition time information from the series. In general, smoothness versus graininess of the liver was used as a method for differentiating poor from moderate quality and image sharpness seen best in thorax at the junction of lung and chest wall was used for differentiating good from moderate quality. The Friedman test was applied for comparative analysis of scores given by the two physicians. The data were assessed for its variation in mean score on

Table 1: Characteristics of the patients

| Patient characteristics | Value |
|--------------------------|--------------------|
| Gender | |
| Male | 21 (52.5) |
| Female | 19 (47.5) |
| Age (years) | 51 \pm 15.3 |
| Weight (kg) | 48.7 \pm 8.6 |
| Height (cm) | 154.7 \pm 8.9 |
| BMI (kg/m ²) | 20.4 \pm 3.7 |
| BMI (kg/m ²) | |
| <18 | 14 (35) |
| 18–25 | 19 (47.5) |
| >25 | 7 (17.5) |
| Preinjected dose | 2.6 \pm 0.5 mCi |
| Postinjected dose | 0.1 \pm 0.06 mCi |
| Net injected dose | 2.5 \pm 0.5 mCi |

Values are presented as mean \pm SD or frequency (%). SD: Standard deviation, BMI: Body mass index

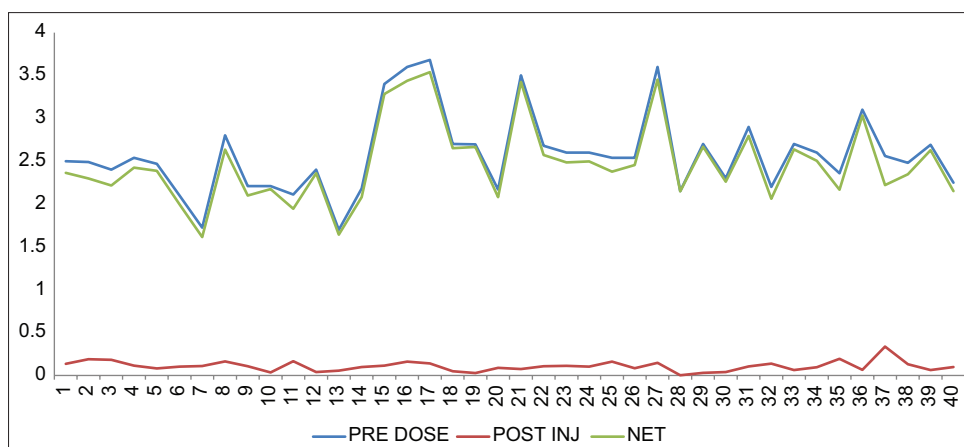


Figure 1: Graphical representation pre, post, and net injected dose in mCi for all patients

Table 2: Qualitative image analysis in Group A and Group B

| Group | Score 1 | Score 2 | Score 3 | Score 4 | Score 5 | Average score |
|----------|---------|-----------|---------|-----------|-----------|---------------|
| A | | | | | | |
| 1 | 3 (7.5) | 21 (52.5) | 12 (30) | 1 (92.5) | - | 2.3±0.7 |
| 2 | - | 1 (2.5) | 14 (35) | 22 (55) | - | 3.6±0.5 |
| 3 | - | - | - | 19 (47.5) | 19 (47.5) | 4.5±0.5 |
| B | | | | | | |
| 1 | 24 (60) | 13 (32.5) | 2 (5) | - | - | 1.4±0.6 |
| 2 | 1 (2.5) | 1 (2.5) | 20 (50) | 17 (42.5) | - | 3.3±0.7 |
| 3 | - | - | - | 7 (17.5) | 32 (80) | 4.8±0.4 |

Values are presented as mean±SD or frequency (%). SD: Standard deviation

different time/bed based on BMI too as reported by two physicians. The study review process was approved by the Institutional Review Board of Mahamana Pandit Madan Mohan Malaviya Cancer Centre, Varanasi, A Unit of Tata Memorial Centre (OIEC/11000714/2024/00001, dated February 1, 2024).

Results

The study experienced data loss from the storage and backup system, resulting in Physician B reporting data for 39 patients. Physician A's evaluations included 37 patients at 1 min per bed, 37 patients at 2 min per bed, and 38 patients at 3 min per bed. The average scores of 1 min/bed, 2 min/bed, and 3 min/bed data by Physician A were 2.3 ± 0.7 , 3.6 ± 0.5 , and 4.5 ± 0.5 and by Physician B were 1.4 ± 0.6 , 3.3 ± 0.7 , and 4.8 ± 0.4 [Table 2]. The Friedman test was performed to compare the qualitative scores between two physicians, which resulted in significant difference in Physician A ($P < 0.000$) and Physician B ($P < 0.000$). Significant differences were observed on comparing the mean score of 1 min/bed ($P = 0.000$) and 3 min/bed data ($P = 0.006$) between Physician A and B and no significant differences was observed on comparing the mean score of 2 min/bed between Physician A and

B ($P = 0.073$). The number of studies assigned with score 4 and 5 by Physician A and Physician B for 3 min/bed image was 19:19 and 7:32, respectively, as shown in Table 2. The maximum score was assigned to images of 3 min/bed, followed by 2 min/bed and worst score was assigned to 1 min/bed data. The scored images (axial fused-PET/CT and maximum intensity projection) are shown in Figure 2a-f. The quantitative image assessments was also done. There were significant differences in SUV_{max} between 1 min, 2 min, and 3 min ($P < 0.000$). On the other hand, there were no significant differences in SUV_{mean} between 1 min/bed, 2 min/bed, and 3 min/bed ($P = 0.378$), as shown in Table 3. Second, a box plots are shown in Figure 3 for comparison of SUV_{max} and SUV_{mean} at different times. The coefficient of variation was observed to be more between Physician A and B in 1 min/bed while the variability was less in 2 min/bed and 3 min/bed image. The scores given by Physician A and B in 3 min was compared between BMI <18 kg/m², 18–25 kg/m², and >25 kg/m² [Figure 4a-c]. For patients with BMI <18 kg/m² and 18–25 kg/m², the mean score given by Physician A and B were 4.5 and 4.8, respectively. For patients with BMI >25 kg/m², the mean score given by Physician A and B was 4.5 (both the cases).

Discussion

The positron emission process is a Poisson distribution phenomenon and PET is a statistical imaging method, wherein noise is inevitable in resulting images.^[17] This can be taken care of by either increasing the count rate through injecting a high amount of activity or increasing the time/bed in PET acquisition. However, both have their own limitations. High activity can lead to increasing count losses and accidental coincidences, whereas long duration acquisition can lead to motion artifacts more frequently.^[17,18] A balanced approach shall be to reduce dose and have the optimal time to obtain best quality image without motion error. In oncology, where follow-up studies are being routinely done under PET-CT for disease management, dose reduction can be a boon to patients. However, similar

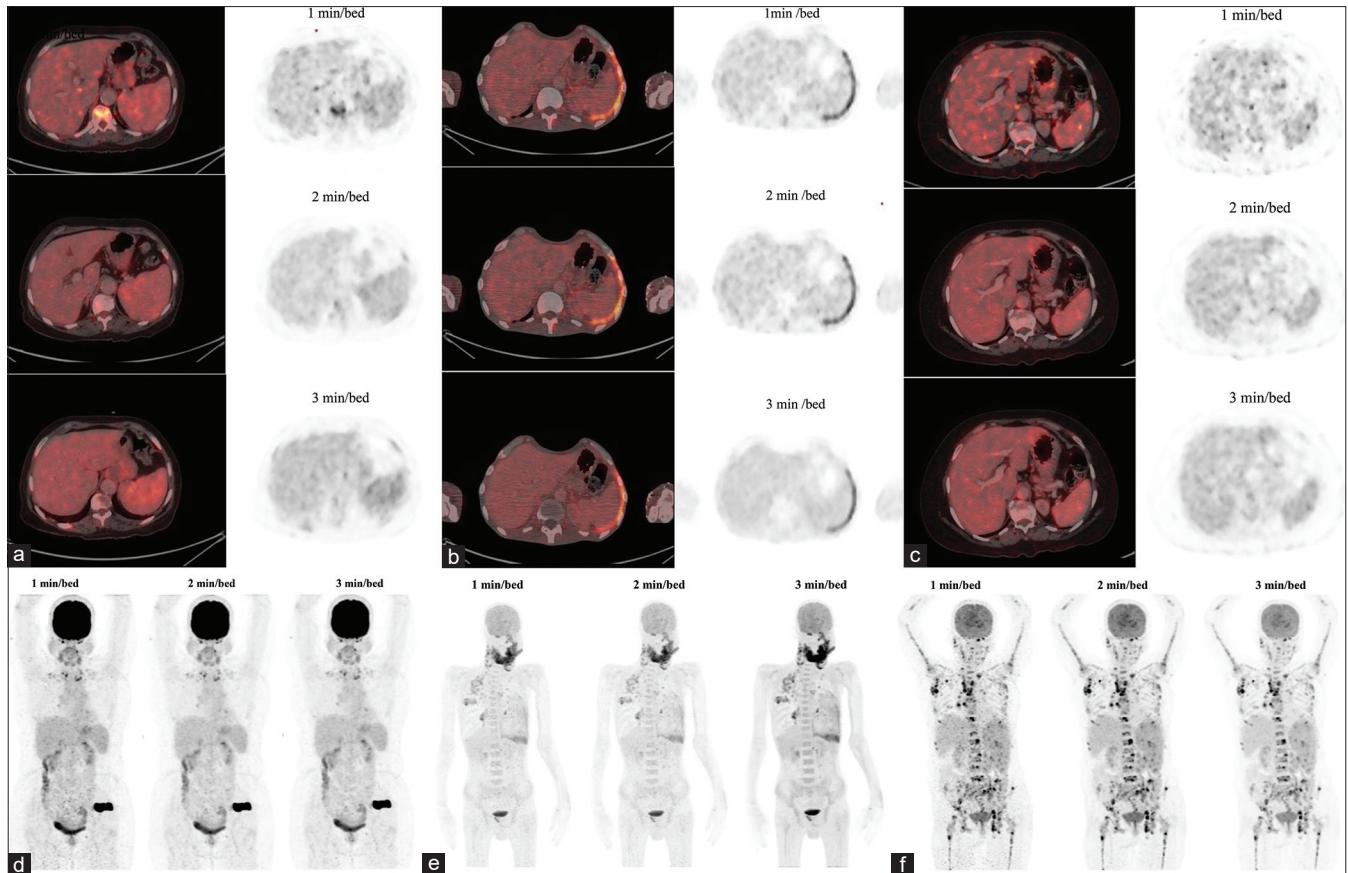


Figure 2: (a) Fused and corresponding positron emission tomography (PET) only image with score assigned as 1, 3, and 4 for 1 min/bed, 2 min/bed, and 3 min/bed axial image of same patient, (b) Fused and corresponding PET only images with score assigned as 2, 4, and 5 for 1 min/bed, 2 min/bed, and 3 min/bed axial image of same patient, (c) Fused and corresponding PET only images with score assigned as 1, 3, and 5 for 1 min/bed, 2 min/bed, and 3 min/bed axial image of same patient, (d) maximum intensity projection (MIP) Images with score assigned as 1, 3, and 4 for 1 min/bed, 2 min/bed, and 3 min/bed of same patient, (e) MIP Images with score assigned as 2, 4, and 5 for 1 min/bed, 2 min/bed, and 3 min/bed of same patient, (f) MIP Images with score assigned as 1, 3, and 5 for 1 min/bed, 2 min/bed, and 3 min/bed of same patient

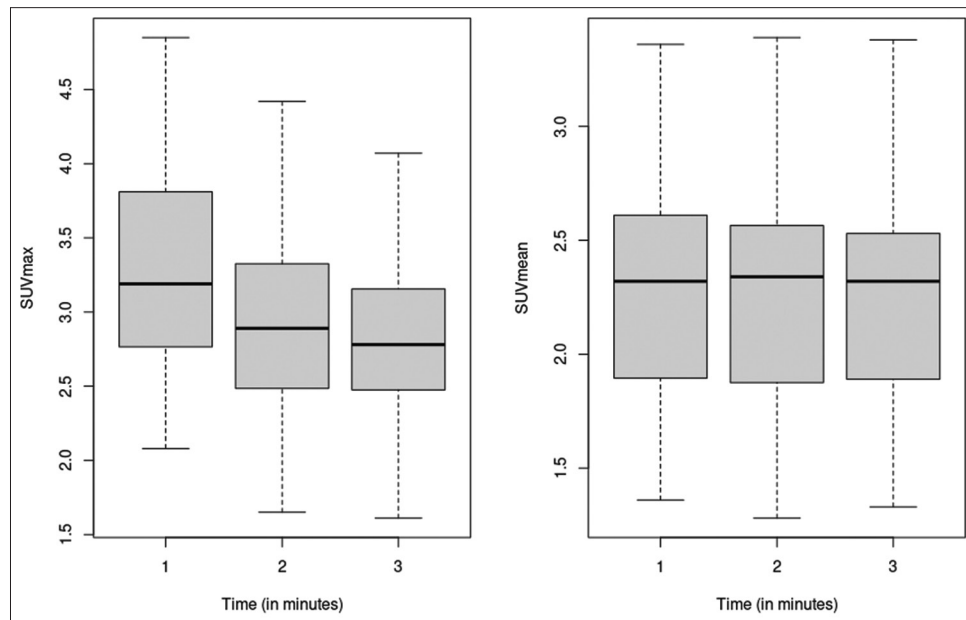


Figure 3: Box plots for comparison of maximum standardized uptake value and mean standardized uptake value among different times. SUV_{max}: Maximum standardized uptake value, SUV_{mean}: Mean standardized uptake value

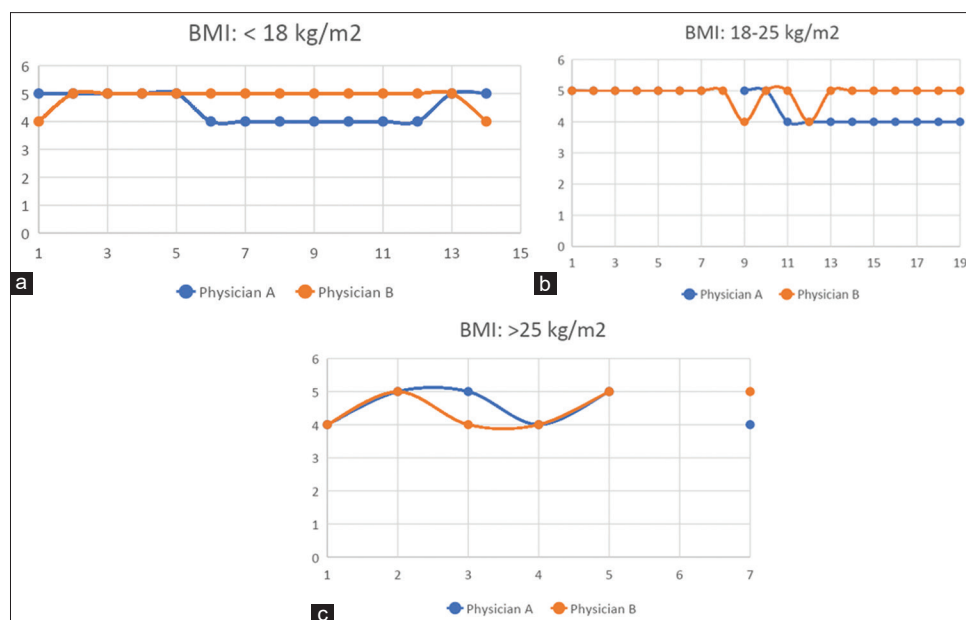


Figure 4: (a-c) Line plots showing the variability between the scores for each patient based on body mass index (<18 vs. 18–25 vs. >25) given by Physician A and B. BMI: Body mass index

Table 3: Quantitative image analysis in Group A and Group B

| Measurement | 1 min | 2 min | 3 min | P |
|---------------------|---------|---------|---------|--------|
| SUV _{max} | 3.3±0.8 | 2.9±0.7 | 2.8±0.6 | 0.000* |
| SUV _{mean} | 2.3±0.5 | 2.2±0.5 | 2.2±0.5 | 0.378 |
| COV (%) | | | | |
| Physician A | 28.78 | 15.55 | 11.26 | |
| Physician B | 41.64 | 19.89 | 8.06 | |

*- $P < 0.0001$, Values are presented as mean±SD. SD: Standard deviation, COV: Coefficient of variation, SUV_{mean}: Mean standardized uptake value, SUV_{max}: Maximum standardized uptake value

optimization of dose for patients with high BMI (>25) to achieve both reduction of effective dose and higher image quality is not useful as shown by Nagaki *et al.*^[19] The dominant physical performance attribute of GE Discovery IQ 5 ring model is its longer crystal depth (30 mm in IQ) and high sensitivity that too in denser material like BGO crystal eventually helping reduce radiation burden.^[14,20] Second, its long axial coverage due to five rings served to positively impact patient experience and scanner throughput at challenging situations like delay of consignment. Many studies have been done previously exploiting the advantage of a long axial FOV (AFOV) PET scanner with AFOV range of 15–30 cm.^[8,10,21-28] The extended FOV feature is now being incorporated in the upcoming digital PET system, as is evident with the latest installation of the EXPLORER model at University of California-Davis.^[29] It is the world's first total body PET scanner with sensitivity as high as 174 kcps/MBq and AFOV of 194.0 cm. In addition to this, the EXPLORER consortium supported the development of Penn PET EXPLORER, which has 64 cm AFOV and sensitivity of 55 cps/kBq.^[30,31] The world

is moving to digitization and that too at a very fast pace, replacing the conventional models. The digital PET system like Biograph Vision model, with improved sensitivity, is able to help reduce scan dose and maintain high contrast in image as mentioned in the work of Suleman Surti *et al.* and Joyce van Sluis *et al.*^[5,22] These models demonstrate substantially huge sensitivity in comparison to conventional analog systems and shall indeed help increase the throughput with a possibility of conducting dynamic studies as well.^[29,32-37] However, cost remains a matter of great concern and GE's Discovery IQ 5 ring, 16-slice PET/CT model currently available in developing countries like ours, serves to be the best solution in molecular imaging taking into consideration the clinical outcome and cost-effectiveness. At our institute, we could reap out benefit from the long axial system amid cases of radiotracer availability challenges by judicious selection of patients which could be covered within 4 bed position and hence manage time and activity both. Second, as the study was conducted under 4-bed position, we were able to avoid motion artifact which could have been evident in long bed/duration acquisition protocol. The 3 min/bed protocol with 0.05 mCi/kg of ^{18}F -FDG as per our institutional protocol proved to be the best in giving highest quality image for clinical reporting, which gradually became grainy and difficult to report with confidence.

Conclusion

This modality with high sensitivity and long axial length (five rings with a span of 26 cm AFOV) can act as a savior for cyclotron dependent high-end centers struggling with the availability of radiotracer. The increased AFOV itself provides large coverage, consequently reducing the

number of beds and eventually scan time. We used the advantage of increased sensitivity by reducing the injecting activity rather than scan time to meet the challenges at our institute, which proved to be a successful one.

Limitations

This is a single-center retrospective qualitative analysis only study. Second, the validation needs to be conducted in larger patient cohorts and studied at multicenter, especially in a prospective trial. The BMI correlation cannot be commented on as we had less no of patients with BMI >25.

Acknowledgment

Authors are thankful to Ms. Ankita Pal, Biostatistician, for her assistance in manuscript.

Financial support and sponsorship

Nil.

Conflicts of interest

There are no conflicts of interest.

References

- Schöder H, Erdi YE, Larson SM, Yeung HW. Pet/ct: A new imaging technology in nuclear medicine. *Eur J Nucl Med Mol Imaging* 2003;30:1419-37.
- Boellaard R, Delgado-Bolton R, Oyen WJ, Giammarile F, Tatsch K, Eschner W, *et al.* FDG PET/CT: EANM procedure guidelines for tumour imaging: Version 2.0. *Eur J Nucl Med Mol Imaging* 2015;42:328-54.
- Petersen H, Holdgaard PC, Madsen PH, Knudsen LM, Gad D, Gravergaard AE, *et al.* FDG PET/CT in cancer: Comparison of actual use with literature-based recommendations. *Eur J Nucl Med Mol Imaging* 2016;43:695-706.
- Surti S. Update on time-of-flight PET imaging. *J Nucl Med* 2015;56:98-105.
- Surti S, Kuhn A, Werner ME, Perkins AE, Kolthammer J, Karp JS. Performance of philips Gemini TF PET/CT scanner with special consideration for its time-of-flight imaging capabilities. *J Nucl Med* 2007;48:471-80.
- Karp JS, Surti S, Daube-Witherspoon ME, Muehllehner G. Benefit of time-of-flight in PET: Experimental and clinical results. *J Nucl Med* 2008;49:462-70.
- Wright CL, Binzel K, Zhang J, Knopp MV. Advanced functional tumor imaging and precision nuclear medicine enabled by digital PET technologies. *Contrast Media Mol Imaging* 2017;2017:5260305.
- Rausch I, Ruiz A, Valverde-Pascual I, Cal-González J, Beyer T, Carrio I. Performance Evaluation of the vereos PET/CT system according to the NEMA NU2-2012 standard. *J Nucl Med* 2019;60:561-7.
- Zhang J, Maniawski P, Knopp MV. Performance evaluation of the next generation solid-state digital photon counting PET/CT system. *EJNMMI Res* 2018;8:97.
- Hsu DFC, Ilan E, Peterson WT, Uribe J, Lubberink M, Levin CS. Studies of a next-generation silicon-photomultiplier-based time-of-flight PET/CT system. *J Nucl Med* 2017;58:1511-8.
- GE-Healthcare. Discovery IQ 5-Ring Low Dose Capabilities, Short Scan Times Deliver Economic Value for Jaslok Hospital; 2016. Available from: <https://www.gehealthcare.com/-/media/d19bf81af4494368b0215bad40e4560a.pdf?la=en&hash=BD020C9D0B3FFC1B2B1198FC8CDE42B537EC4E6E>. [Last accessed on 2024 Aug 22, Last updated on 2024 Mar 01].
- Kajisako M, Kawase S, Mitsumoto K, Tatsuno K, Higashimura K, Nakamoto Y, *et al.* Performance evaluation of the Bayesian Penalized Likelihood Reconstruction Algorithm Q.Clear on BGO PET/CT system, according to NEMA NU2-2012 standard. *J Nucl Med* 2016;57 Suppl 2:2627.
- Morzenti S, De Ponti E, Guerra L, Zorz A, Landoni C, Crivellaro C, *et al.* Performance evaluation of the discovery IQ-GE PET/CT scanner according to NEMA NU2-2012 standard. *J Nucl Med* 2015;56 Suppl 3:1846.
- Jha A, Mithun S, Singh A, Purandare N, Shah S, Agrawal A, *et al.* NEMA NU-2 2012 performance evaluation of discovery IQ: A high sensitivity PET System. *J Nucl Med* 2015;56 Suppl 3:1847.
- Melcher CL. Scintillation crystals for PET. *J Nucl Med* 2000;41:1051-5.
- Wyrzykowski M, Siminiak N, Kaźmierczak M, Ruchała M, Czepczyński R. Impact of the Q.Clear reconstruction algorithm on the interpretation of PET/CT images in patients with lymphoma. *EJNMMI Res* 2020;10:99.
- Watson CC, Casey ME, Bendriem B, Carney JP, Townsend DW, Eberl S, *et al.* Optimizing injected dose in clinical PET by accurately modeling the counting-rate response functions specific to individual patient scans. *J Nucl Med* 2005;46:1825-34.
- Everaert H, Vanhove C, Lahoutte T, Muylle K, Caveliers V, Bossuyt A, *et al.* Optimal dose of ¹⁸F-FDG required for whole-body PET using an LSO PET camera. *Eur J Nucl Med Mol Imaging* 2003;30:1615-9.
- Nagaki A, Onoguchi M, Matsutomo N. Patient weight-based acquisition protocols to optimize (18) F-FDG PET/CT image quality. *J Nucl Med Technol* 2011;39:72-6.
- Pan T, Einstein SA, Kappadath SC, Grogg KS, Lois Gomez C, Alessio AM, *et al.* Performance evaluation of the 5-Ring GE discovery MI PET/CT system using the national electrical manufacturers association NU 2-2012 Standard. *Med Phys* 2019;46:3025-33.
- Conti M, Bendriem B, Casey M, Eriksson L, Jakoby B, Jones WF, *et al.* A high-throughput whole-body PET scanner using flat panel PS-PMTs. Vol. 4; 2003. p. 2442-6.
- van Sluis J, de Jong J, Schaar J, Noordzij W, van Snick P, Dierckx R, *et al.* Performance of a high sensitivity PET scanner based on LSO panel detectors. *IEEE Trans Nucl Sci* 2006;53:1136-42.
- van Sluis J, de Jong J, Schaar J, Noordzij W, van Snick P, Dierckx R, *et al.* Performance characteristics of the digital biograph vision PET/CT system. *J Nucl Med* 2019;60:1031-6.
- Jakoby BW, Bercier Y, Conti M, Casey ME, Bendriem B, Townsend DW. Physical and clinical performance of the mCT time-of-flight PET/CT scanner. *Phys Med Biol* 2011;56:2375-89.
- Bettinardi V, Presotto L, Rapisarda E, Picchio M, Gianolli L, Gilardi MC. Physical performance of the new hybrid PET/CT discovery-690. *Med Phys* 2011;38:5394-411.
- Kolthammer JA, Su KH, Grover A, Narayanan M, Jordan DW, Muzic RF. Performance evaluation of the ingenuity TF PET/CT scanner with a focus on high count-rate conditions. *Phys Med Biol* 2014;59:3843-59.
- Delso G, Fürst S, Jakoby B, Ladebeck R, Ganter C, Nekolla SG, *et al.* Performance measurements of the siemens mMR integrated whole-body PET/MR scanner. *J Nucl Med* 2011;52:1914-22.
- Grant AM, Deller TW, Khalighi MM, Maramraju SH, Delso G, Levin CS. NEMA NU 2-2012 performance studies for the SiPM-

- based ToF-PET component of the GE SIGNA PET/MR system. *Med Phys* 2016;43:2334.
29. Spencer BA, Berg E, Schmall JP, Omidvari N, Leung EK, Abdelhafez YG, *et al.* Performance evaluation of the uEXPLORER total-body PET/CT scanner based on NEMA NU 2-2018 with additional tests to characterize PET scanners with a long axial field of view. *J Nucl Med* 2021;62:861-70.
 30. Pantel AR, Viswanath V, Daube-Witherspoon ME, Dubroff JG, Muehllehner G, Parma MJ, *et al.* PennPET explorer: Human imaging on a whole-body imager. *J Nucl Med* 2020;61:144-51.
 31. Karp JS, Viswanath V, Geagan MJ, Muehllehner G, Pantel AR, Parma MJ, *et al.* PennPET explorer: Design and preliminary performance of a whole-body imager. *J Nucl Med* 2020;61:136-43.
 32. Prenosil GA, Sari H, Fürstner M, Afshar-Oromieh A, Shi K, Rominger A, *et al.* Performance characteristics of the biograph vision quadra PET/CT system with a long axial field of view using the NEMA NU 2-2018 standard. *J Nucl Med* 2022;63:476-84.
 33. Alberts I, Hünermund JN, Prenosil G, Mingels C, Bohn KP, Viscione M, *et al.* Clinical performance of long axial field of view PET/CT: A head-to-head intra-individual comparison of the biograph vision quadra with the biograph vision PET/CT. *Eur J Nucl Med Mol Imaging* 2021;48:2395-404.
 34. Alberts I, Schepers R, Zeimpekis K, Sari H, Rominger A, Afshar-Oromieh A. Combined [68 Ga]Ga-PSMA-11 and low-dose 2-[18F]FDG PET/CT using a long-axial field of view scanner for patients referred for [177Lu]-PSMA-radioligand therapy. *Eur J Nucl Med Mol Imaging* 2023;50:951-6.
 35. Wu Y, Feng T, Zhao Y, Xu T, Fu F, Huang Z, *et al.* Whole-body parametric imaging of (18)F-FDG PET using uEXPLORER with reduced scanning time. *J Nucl Med* 2022;63:622-8.
 36. Tan H, Sui X, Yin H, Yu H, Gu Y, Chen S, *et al.* Total-body PET/CT using half-dose FDG and compared with conventional PET/CT using full-dose FDG in lung cancer. *Eur J Nucl Med Mol Imaging* 2021;48:1966-75.
 37. Cherry SR, Jones T, Karp JS, Qi J, Moses WW, Badawi RD. Total-body PET: Maximizing sensitivity to create new opportunities for clinical research and patient care. *J Nucl Med* 2018;59:3-12.